

# INFLUENCE OF THE ADHESION FORCE AND STRAIN HARDENING COEFFICIENT OF THE MATERIAL ON THE RATE OF ADHESIVE WEAR IN A DRY TANGENTIAL FRICTIONAL CONTACT

A. V. Dimaki,<sup>1</sup> I. V. Dudkin,<sup>1</sup> V. L. Popov,<sup>2,3</sup> and E. V. Shilko<sup>1,3</sup>

UDC 539.61: 539.621: 001.891.573

*In the paper, we consider the tangential contact of single microasperities of the interacting surfaces the mechanical characteristics of which are close to the characteristics of typical rail steels. Using computer simulation by the method of discrete elements, we study the influence of the parameters of adhesive interaction of both external and internal surfaces on the regime of wear of asperities. It has been established that with increasing adhesion work, the wear regime changes from slipping (low wear) to grinding or brittle fracture of asperities (high wear), and this change is of threshold nature. An empirical sigmoid dependence of the location of the boundary between the two wear regimes (namely, the threshold value of the adhesive stress) on the value of the material hardening coefficient has been established. It is shown that the logistic nature of this dependence is due to the competition of two mechanisms of elastic strain energy dissipation, which determine the wear regime. These are plastic deformation and adhesion of the contacting surfaces. Special discussion is devoted to the influence of the scale factor on the threshold values of the mechanical characteristics of the material which provide the change of the wear regime.*

**Keywords:** adhesive contact, fracture, wear regimes, computer simulation, discrete elements.

## INTRODUCTION

In the case of dry friction, the surfaces of materials on contact spots undergo wear characterized by complex profiles of microasperities [1–4]. The wear dynamics is determined by a wide range of physical and chemical mechanisms realized on various time and size scales. Accordingly, in addition to the loading conditions, the rate of surface wear is determined by a complex of physical-mechanical parameters of contacting materials and sizes and shapes of microasperities. The above-listed factors determine the stress-strain state of the material of the contact area and the conditions of reaching the critical state in which fragments of the material are separated, that is, wear occurs.

One of the key factors determining the wear rate is the adhesive interaction of materials on contact spots of microasperities [1, 5–7]. Despite a great number of works devoted to a study of various aspects of adhesive wear, the most important laws of wear established by the present time are empirical in character [8–10]. Moreover, the local processes on contact spots of microasperities that determine the character and rate of wear have widely been discussed until now. This caused great interest in the theoretical study of laws of interaction of *structural surface elements* (microasperities) in tangential contact [3, 11, 12]. These studies were focused on revealing and generalizing the conditions of realization of specific wear regimes on the most fundamental scale of microasperities.

---

<sup>1</sup>Institute of Strength Physics and Materials Science of the Siberian Branch of the Russian Academy of Sciences, Tomsk, Russia, e-mail: dav@ispms.tsc.ru; pokrovitelchar@mail.ru; shilko@ispms.tsc.ru; <sup>2</sup>Technische Universität, Berlin, Germany, e-mail: v.popov@tu-berlin.de; <sup>3</sup>National Research Tomsk State University, Tomsk, Russia. Translated from *Izvestiya Vysshikh Uchebnykh Zavedenii, Fizika*, No. 8, pp. 84–94, August, 2019. Original article submitted June 25, 2019.

Rabinovich [13] analytically derived the criterion for separation of a microasperity from ideally plastic material, including the specific adhesion work and the characteristic size of microasperities. The criterion defines conditions of transition from the regime of practically wearless relative slipping of contacting surfaces (plastic smoothing of microasperities [14, 15]) to the regime of forming the so-called *third body* consisting of wear particles [10, 13]. Recent results of numerical study of nano-sized microasperities have demonstrated that despite the adequacy of analytical estimates, the dependence of the wear rate of microasperities on the material parameters can have much more complicated nonlinear character [11, 12]. In particular, this is due to the phenomenon of localization of inelastic shear strain on the contact spot of microasperities that changes qualitatively the character of their interaction.

The purpose of the present work is the determination of conditions of realization of different adhesive wear regimes of microasperities on micro- and mesoscales. On these scales, the mechanical characteristics that determine the plasticity and strength of materials depend significantly on specific features of their internal structure; therefore, direct transfer of results of atomistic computer simulation [16, 17] from nano- to larger scales is problematic.

Within the framework of investigations performed in this work, the influence of the integral (macroscopic) material parameters is analyzed. Among these parameters are the surface adhesion force, yield strength of the material, strain hardening coefficient, and local friction coefficient that characterize relaxation of local stresses and dissipation of elastic energy on lower-lying scales. Elucidation of conditions for realization of specific microasperity wear regimes in terms of these parameters provides the basis required for the construction of macroscopic models and wear criteria possessing high predictability.

At present one of the methods of computer simulation widely used in theoretical analysis of deformation and fracture of materials as well as of contact interaction on the mesoscale level is the discrete element method [18–20]. In the present work, this method is used to study the regimes of adhesive wear of microasperities in dry tangential contact.

## 1. DESCRIPTION OF THE MATHEMATICAL MODEL

Computer simulation was carried out for 2D problem formulation using the discrete element method (DEM). The original formulation of the method called the movable cellular automation (MCA) method [21–23] was used. To describe deformation and fracture of microasperities within the framework of the MCA method, the mechanical model of isotropic elastoplastic materials was constructed. It was based on the following basic assumptions.

1) Discrete elements interact mechanically via flat faces (interaction surfaces) [18, 19]. The model is an analog of the contact *flat-joint* model widely used in traditional DEM realizations used for computer simulation of a solid body [24]. Within the limits of the model, the vector of the interaction force of pair elements is subdivided into the radial (normal) and tangential (shear) components characterized by the specific normal and shear stress components:

$$\begin{cases} \sigma_{ij} = F_{ij}^n / S_{ij}, \\ \tau_{ij} = F_{ij}^\tau / S_{ij}, \end{cases} \quad (1)$$

where  $F_{ij}^n$  and  $F_{ij}^\tau$  are the normal and tangential components of the force vector of the interaction between elements  $i$  and  $j$  ( $F_{ij} = F_{ij}^n + F_{ij}^\tau$ ) and  $S_{ij}$  is the contact area of the pair  $i-j$ . The contact area of the undeformed pair  $S_{ij}^0$  is determined by local packing of discrete elements. For dense packing of elements of the same size  $R$  on the plane used in the present work,  $S_{ij}^0 = 2Rh/\sqrt{3}$ , where  $h$  is the element size in the direction transverse to the plane [22].

2) According to the most widespread DEM formulation [19, 25], when solving the equations of motion in the 2D problem formulation, the discrete element is approximated by the so-called equivalent disk. The given approach allows simplified formulation of the Newton–Euler equations of motion of the elements and consideration of radial and tangential interaction forces as formally independent from each other:

$$\begin{cases} m_i \frac{d^2 \mathbf{r}_i}{dt^2} = m_i \frac{d\mathbf{v}_i}{dt} = \sum_{j=1}^{N_i} (\mathbf{F}_{ij}^n + \mathbf{F}_{ij}^\tau), \\ J_i \frac{d\boldsymbol{\omega}_i}{dt} = \sum_{j=1}^{N_i} \mathbf{M}_{ij}. \end{cases} \quad (2)$$

Here  $\mathbf{r}_i$ ,  $\mathbf{v}_i$ , and  $\boldsymbol{\omega}_i$  are the radius-vector, velocity vector, and angular velocity pseudo-vector of element  $i$ ,  $m_i$  is the mass of the element  $i$ ,  $J_i$  is the moment of inertia of the equivalent disk,  $\mathbf{M}_{ij}$  is the tangential force moment, and  $N_i$  is the number of interacting neighbors of element  $i$ .

3) According to the MCA method, the discrete element is considered as uniformly deformed. Its stress-strain state is characterized by average stress,  $\boldsymbol{\sigma}_{\alpha\beta}$ , and strain,  $\boldsymbol{\varepsilon}_{\alpha\beta}$ , tensors. The components of these tensors are calculated in terms of forces of interaction of the element with its neighbors as well as of the radial and shear strains in pairs [21, 22]. In particular,

$$\sigma_{\alpha\beta}^i = \frac{R_i}{\Omega_i} \sum_{j=1}^{N_i} S_{ij}^0 \left[ \sigma_{ij} (\mathbf{n}_{ij})_\alpha (\mathbf{n}_{ij})_\beta + \tau_{ij} (\mathbf{n}_{ij})_\alpha (\mathbf{t}_{ij})_\beta \right], \quad (3)$$

where  $\alpha, \beta = x, y, z$  ( $XYZ$  is the laboratory system of coordinates),  $\Omega_i$  is the element of volume  $i$ , and  $(\mathbf{n}_{ij})_\alpha$  and  $(\mathbf{t}_{ij})_\alpha$  are projections of the unit normal and tangential vectors, defined on the contact area of pair  $i-j$ , onto the  $\alpha$  axis of the laboratory system of coordinates. The components of the average strain vector are calculated analogously.

4) The deformability of elements in calculation of the interelement interaction is taken into account within the limits of the multiparticle formulation of the interaction forces of the elements. In the present work, the material of the discrete element was assumed isotropic and elastoplastic, and its elastic mechanical behavior obeyed to generalized Hook's law. The corresponding multiparticle expressions for the radial and tangential force components of the response of element  $i$  to the mechanical action from element  $j$  have the following form [21, 22]:

$$\begin{cases} \sigma_{ij} = 2G_i \varepsilon_{ij} + (1 - 2G_i/3K_i) \sigma_{\text{mean}}^i, \\ \tau_{ij} = G_i \gamma_{ij}, \end{cases} \quad (4)$$

where  $G_i$  and  $K_i$  are the shear modulus and the omnidirectional compression modulus of the material of element  $i$ ,  $\sigma_{\text{mean}}^i = (\sigma_{xx}^i + \sigma_{yy}^i + \sigma_{zz}^i)/3$  is the average stress in the bulk of element  $i$ ,  $\varepsilon_{ij}$  and  $\gamma_{ij}$  are the normal and shear strain components of element  $i$  of pair  $i-j$ . As a criterion for the onset of the plastic flow, the von Mises criterion was used:

$$\sigma_{eq}^i = \sigma_y(\varepsilon_{\text{plast}}), \quad (5)$$

where  $\sigma_{eq}^i$  is the stress intensity in the volume element,  $\sigma_y(\varepsilon_{\text{plast}})$  is the critical stress whose value depends on the plastic strain  $\varepsilon_{\text{plast}}$  accumulated in the element. The model of the plastic flow is realized within the limits of the MCA method with the use of the adapted Wilkins algorithm [26]. Details of its numerical realization are given in [21, 22].

5) The pairs of elements that model the areas of consolidated material are chemically bound. The local fracture is modeled by breaking a chemical bond in the pair (which corresponds to the formation of a local crack). The condition of bond breaking is described by the fracture criterion. In the present work, the von Mises criterion [21, 22]:

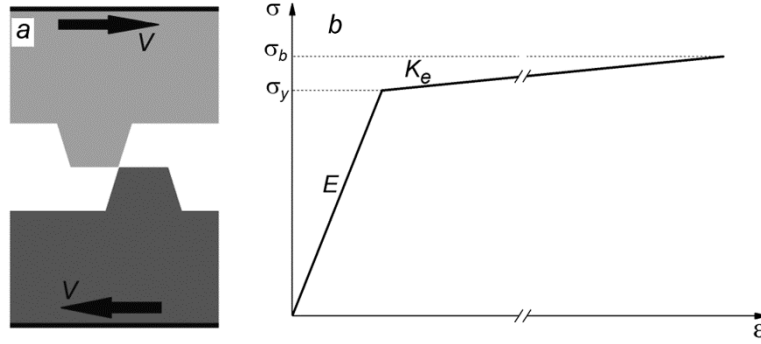


Fig. 1. Schematic of the computer model (a) and diagram of loading of the model material of microasperities (b).

$$\sigma_{eq} = \sigma_b \quad (6)$$

was used as the criterion for breaking the bond in a pair of elements, where  $\sigma_b$  is the tensile strength of the chemical bond in the pair.

The contact interaction is possible between unbounded elements, including the compressive strength in the direction perpendicular to the plane of contact (repulsion of the elements) and the slipping strength in the contact plane (dry friction). Details of the dry friction model implementation are given in [19], the model parameter to be assigned is the dry friction coefficient  $\mu$ . Note that within the framework of the given model of contact interaction, the possibility of *cold welding* of surfaces that can be realized only under condition of chemical degree of purity and atomic smoothness of the surfaces is disregarded.

6) The interaction of unbounded elements is adhesive, that is, the attractive radial force defined as the derivative of the adhesive potential acts between the elements without mechanical contact of their surfaces [27, 28]. In this work, we used the simplified Dugdale formulation of such potential [29, 30]: the attraction force was constant for the entire length of action of the potential (before reaching a preset maximal distance  $\delta$  between the surfaces). In this case, the force of tangential interaction of chemically unbounded non-contacting elements is set equal to zero. Accordingly, the pair of unbounded non-contacting elements interacts with constant attractive radial force  $F_{adh}$  if the distance between the surfaces of the elements does not exceed  $\delta$ :

$$F_{ij}^n = F_{adh} = \sigma_0 S, \quad (7)$$

where  $S$  is the surface contact area of the elements. The specific force  $\sigma_0$  is the material parameter for the pair of interacting materials. The specific adhesion work (surface energy) is defined as  $w_a = \sigma_0 \delta$ , where  $\sigma_0$  is the adhesion stress.

## 2. PROBLEM FORMULATION AND RESULTS OF COMPUTER SIMULATION

The tangential contact of two microasperities made of an elastoplastic material and having trapezoid shapes and the same sizes was considered (Fig. 1a). The heights of microasperities were  $D = 0.5$  mm (500  $\mu\text{m}$ ), and the size of the discrete element was  $d = 0.025$  mm (25  $\mu\text{m}$ ). The physical-mechanical properties of the model material of contacting surfaces were close to the properties of rail steel: the density was  $\rho = 7800$  kg/m<sup>3</sup>, the Young modulus was  $E = 206$  GPa, the Poisson coefficient was  $\nu = 0.28$ , the elastic limit was  $\sigma_y = 600$  MPa, the strain hardening coefficient was set constant (linear strain hardening) and equal to  $K_e \approx 1200$  MPa, and the tensile strength was  $\sigma_b = 920$  MPa. The

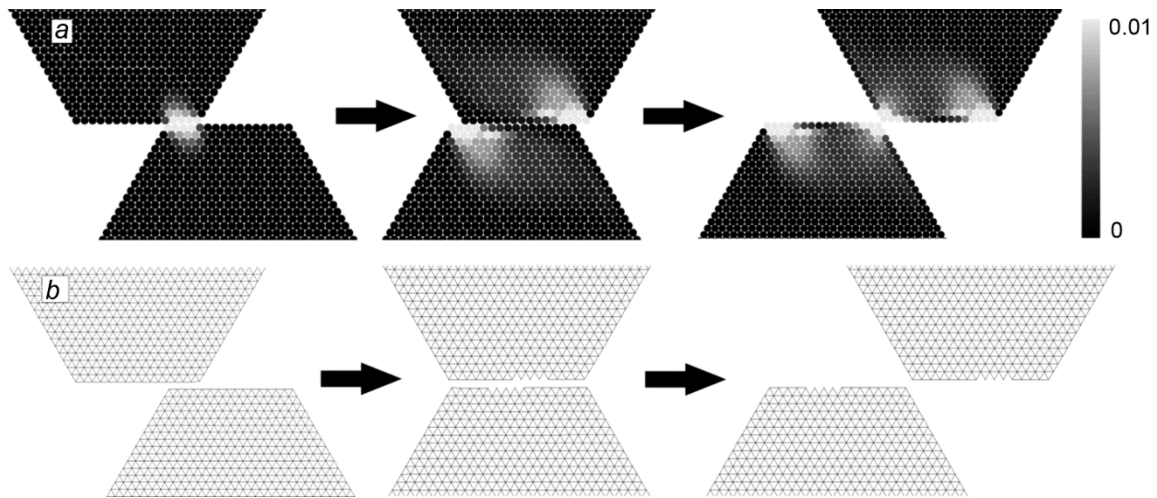


Fig. 2. Evolution of the structure (a) and system of interelement bonding of microasperities (b) in the regime of low wear (slippage) of microasperities. Here *a* shows the grayscale image of the distribution of the plastic deformation intensity and *b* indicates locations of the centers of mass of the elements; straight line segments connecting them show chemically bonded pairs of elements.

uniaxial loading diagram of the material used in our work is schematically shown in Fig. 1*b*. According to the theoretical assumptions of the model described above, we suppose that the adhesion force described by the Dugdale model acts between the unbounded fragments of the material. The length of action of the adhesive potential was  $\delta = 1$  nm. The dry friction coefficient of the contacting surfaces  $\mu$  was set equal to zero unless specially indicated.

The external surfaces of the contacting materials moved relative to each other in the horizontal direction with a constant velocity  $V$  (Fig. 1*a*). The vertical arrangement of these surfaces was fixed, thereby providing the fulfillment of conditions of tangential contact of microasperities. The periodic boundary conditions were assigned on the left and right system boundaries. The microasperity surfaces had regular profile with geometrical characteristics of the microasperities defined by the size of the discrete element. The initial location of microasperities was such that their overlap by  $2R/\sqrt{3}$  was provided that corresponded to the low-angle regime of contact interaction.

A single event of interaction of microasperities was simulated. The character of the fracture and wear of microasperities was analyzed at different adhesion stresses  $\sigma_0$ . Results of computer simulation have allowed us to reveal two characteristic wear regimes called *low* and *high* wear regimes below.

The low wear regime [3, 11] is characterized by accumulation of inelastic strain in upper layers of the material of contacting microasperities and damage of them without separation of material fragments (at least, for a single slip of microasperities, Fig. 2). In spite of the fact that multiple slip of microasperities can lead to their fracture as a result of gradual accumulation of damages, the value of the effective wear coefficient was sufficiently small in this regime.

In the high wear regime [11, 12], even single contacts of microasperities led to separation of wear particles and fracture of microasperities or their complete separation from the base (Fig. 3). It is obvious that in this interaction regime, the wear coefficient is significantly higher than in the previous case.

The above-described difference of the characters of interaction and wear of microasperities justifies the need for elucidating the parameters that determine the qualitative change of the wear rate. Results of computer simulation showed that the qualitative change of the character of interaction of microasperities in tangential contact (from almost wearless slip to fracture leading to high wear) occurs with increasing adhesion stress of the contacting surfaces (the  $\sigma_0$  value) and has a threshold character. The interaction of microasperities without their wear takes place at relatively small values of the adhesion stress  $\sigma_0$  not exceeding its threshold value  $\sigma_0^*$ . For  $\sigma_0 > \sigma_0^*$ , the interaction of microasperities is accompanied by their fracture caused by *grinding* of the surface layers (Fig. 3), fragmentation of microasperities, or

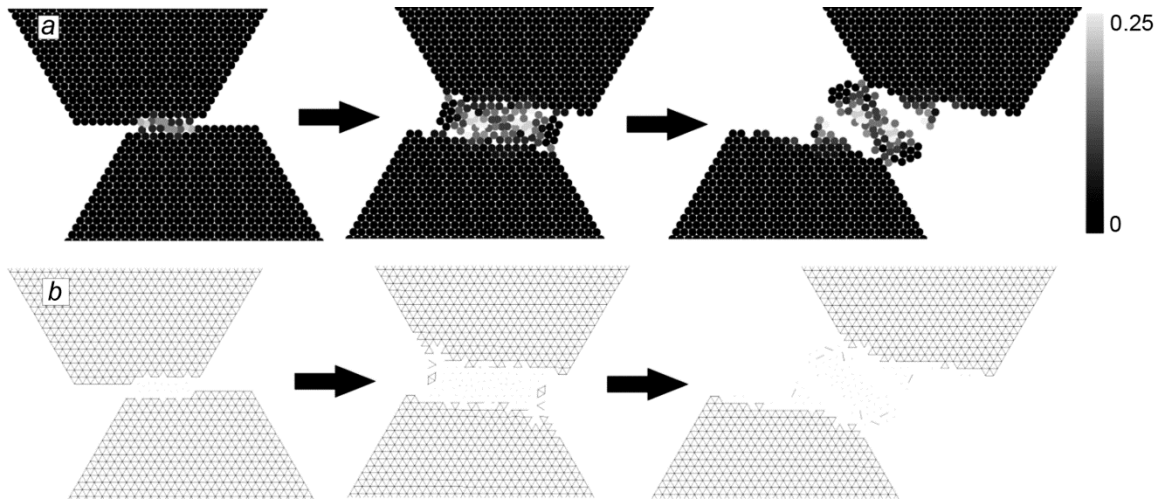


Fig. 3. Evolution of the structure (a) and system of interelement bonding (b) in the regime of high wear of microasperities. The designations are the same as in Fig. 2.

their separation from the base [31]. Thus, the adhesion stress can be considered as the parameter determining the wear regime with tangential contact of microasperities. The following physical explanation can be given to the threshold character of the adhesion stress.

The increase of the stresses and their gradients in the volume of microasperities during their contact interaction causes the involvement of energy dissipation channels on various scales, from those of atoms to microasperities [32]. The first dissipation channel is associated with generation and evolution of crystal lattice defects providing the integral macroscopic plasticity of the material. An important characteristic of this channel is the elastic energy dissipation power characterized, in particular, by the strain hardening coefficient of the material  $K_e$ . The channel provides preservation of the continuity of microasperities during deformation, and its dissipative ability defines the possibility of wearless contact interaction.

The second dissipation channel realized at a higher scale level in comparison with the first channel is associated with local fracture of the microasperity material. The important characteristics of this channel are the strength  $\sigma_b$  and the critical (fracture) value of the accumulated elastic energy density of the material  $w_{\text{elast}}^{\text{crit}} = \sigma_b^2 / 2E$ . The channel is involved when the possibilities of the first dissipation channel (plastic deformation) have been exhausted and the local stress reaches its critical value. The involvement of the dissipation channel associated with fracture makes realization of the regime with high wear rate possible.

The involvement of the second channel (in particular, damages of the contact surfaces, Fig. 2) is necessary but insufficient condition of transition to the regime of intense wear. The involvement of the third dissipation channel associated with adhesive interaction (attraction) of the initial surface fragments and fragments newly formed as a result of local fracture of surface fragments at distances less than  $\delta$  is a key factor of such transition. Two aspects defining the influence of the given channel can be distinguished. First, the attraction of the surface fragments prevents slipping of microasperities, thereby providing effective strain hardening of the contact surface. Under conditions of forced strain, this promotes the involvement of dissipation channels associated with plastic deformation and local fracture not only directly on the contact surface of microasperities, but also in the subsurface layers. This may be accompanied by the formation of localized shear bands in the contact area of microasperities [11, 12]. Second, the surface adhesion makes the separation of fragments of these layers (or the entire surface layer) from microasperities possible, with their subsequent adhesion to the opposite surface, motion together with this surface, repeated adhesion to the initial microasperities or to other material fragments, etc. All processes described above are realized during intense wear. An important energy characteristic of this dissipation channel is the elastic energy density  $w_{\text{attract}} = (\sigma_0)^2 / 2E$  that can be accumulated by contacting surface layers of the material in tension due to their adhesion.

It is obvious that the intense wear regime is much more energetically expensive in comparison with the wearless slip regime at which the contact surfaces of microasperities undergo plastic (mainly shear) deformation. Therefore, the intense wear regime with tangential contact can be realized if the adhesive interaction of surfaces achieves a certain minimal (threshold) energy  $w_{\text{attract}} = w_{\text{attract}}^* = (\sigma_0^*)^2 / 2E$ . Since the necessary condition for the intense wear of microasperities is their damaging and cracking, the threshold value  $w_{\text{attract}}^*$  is directly proportional to  $w_{\text{elast}}^{\text{crit}}$ . In terms of the energy characteristics, there is a threshold value of the ratio  $\sigma_0/\sigma_b$  such that for  $\sigma_0 \leq \sigma_0^*$ , the wearless slipping of surfaces is realized, and for  $\sigma_0 > \sigma_0^*$ , the intense wear regime is observed.

The  $\sigma_0^*$  value subdividing the regimes of the wearless friction and the friction with intense wear is a function of the linear size  $L$  of microasperities and of the mechanical characteristics of the material defining the conditions and intensity of involvement of the dissipation channels. The foregoing determines the urgency of a parametric study of the influence of sizes and mechanical characteristics of the interacting microasperities on the threshold adhesion stress  $\sigma_0^*$  at which qualitative changes of the wear regime are observed.

### 2.1. Influence of the microasperity scale on the wear regime

One of the factors that determines the degree of influence of the adhesion on the wear regime is the ratio of the microasperity size  $L$  to the length of action of adhesive potential  $\delta$ . This fact was first pointed out by Rabinovich in [13] where he demonstrated that the character of wear is determined by the ratio of the work of adhesion forces to the maximal elastic energy that can be accumulated in the volume of microasperities. Note that in [13] and recent works [3, 12, 14], the influence of the magnitude of the adhesion work has been studied, whereas the influence of the length of action of the adhesive potential  $\delta$  has been disregarded. In this connection, in the present work we study dependences of the fracture regime of microasperities in tangential contact on the adhesion stress  $\sigma_0$  at fixed values of  $L$  and  $\delta$ . The sizes of microasperities varied from 500 to 0.05  $\mu\text{m}$ , and the length of action of the adhesive potential varied from 1 nm to 50  $\mu\text{m}$ . In all cases under study, the condition of relatively small values of the length of the adhesive potential was satisfied:  $L < 0.1\delta$ .

Results of computer simulation showed that for all examined values of  $L$  and  $\delta$ , both wear regimes described above were realized, including the low wear for  $\sigma_0 \leq \sigma_0^*$  and the high wear for  $\sigma_0 > \sigma_0^*$ . Of principal importance is the result that the location of the threshold point  $\sigma_0^*$  was determined by the ratio  $L/\delta$  rather than by absolute values of  $L$  and  $\delta$  (Fig. 4). From the figure it can be seen that with increasing ratio  $L/\delta$ , the minimal value of the adhesion stress at which the intense wear can be realized increases. The dependence  $\sigma_0^*(L/\delta)$  is nonlinear in character and reaches a constant value for the ratio  $L/\delta$  lying in the range  $10^4$ – $10^5$ .

The above-described size effect is explained based on the ratio of the work of elastic energy accumulated by deformed microasperities to the work of adhesion force. To within a constant factor, this ratio can be written in the following form:

$$\frac{W_{\text{adh}}}{W_{\text{elast}}^{\text{crit}}} = \frac{w_{\text{adh}} S_{\text{cont}}}{w_{\text{elast}}^{\text{crit}} V_{\text{asp}}} \approx \frac{\sigma_0 \delta E}{(\sigma_c)^2 L}, \quad (8)$$

where  $S_{\text{cont}}$  is the surface area of the contact of microasperities, and  $V_{\text{asp}}$  is the microasperity volume. The larger the ratio  $W_{\text{adh}}/W_{\text{elast}}^{\text{crit}}$ , the more energetically favorable are the conditions for realization of the regime of high wear of microasperities. The value of the ratio given by Eq. (8) increased with decreasing microasperity size or increasing  $\delta$  that qualitatively explains the established character of the dependence of the critical adhesion stress  $\sigma_0^*$  on the size factor.

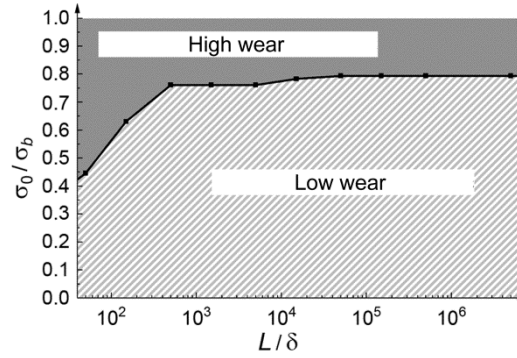


Fig. 4. Dependence of the location of the boundary between the regimes of the low wear and high wear of microasperities on the ratio of the size  $L$  of microasperities to the length of action of the Dugdale potential  $\delta$ . Dots show the threshold values  $\sigma_0^* / \sigma_c$  from the results of computer simulation.

Note that for the basic value of 1 nm taken in our calculations for the length of the adhesive potential (which corresponds to the *limiting* case of atomically smooth surfaces), the characteristic scale of microasperities at which the curve  $\sigma_0^*(L/\delta)$  for the material considered in the work is saturated was several ten micrometers. For the microasperities of larger size, the results of analysis of the wear regimes can be considered scale invariant (for scale invariant mechanical characteristics of the material). The results presented below refer to the microasperities whose sizes provide the fulfillment of the scale invariance condition.

## 2.2. Influence of the mechanical characteristics of the material on the wear regime

The mechanical characteristics of the material of the surface layers have a decisive influence on the location of the boundary (the  $\sigma_0^*$  value) between the areas of *high* and *low* wear, first of all, on the characteristics that determine the elastic energy dissipation power. Among them, the strain hardening coefficient  $K_e$  is the key value, since the dissipation channel associated with plastic deformation is involved in all regimes of interaction of microasperities. The foregoing stimulated a parametric study of the influence of this parameter on the threshold  $\sigma_0^*$  value.

Results of computer simulation showed that the dependence  $\sigma_0^*(K_e)$  has vividly pronounced nonlinear logistic character and is described with good accuracy by a sigmoid function (Fig. 5a). As can be seen from Fig. 5a, for low  $K_e < 0.01E$ ,  $\sigma_0^*$  reaches maximal values ( $0.7\sigma_b - 0.8\sigma_b$ ) and is almost constant. When  $K_e$  increases to  $K_e \approx 0.01E$ , the location of the boundary of transition from the *low* to *high* wear starts at smaller  $\sigma_0^*$  values, that is, the *high* wear is observed for weaker adhesive interaction. At relatively high values of the strain hardening coefficient  $K_e > 0.1E$ , the intense wear regime is realized already at sufficiently small values of the adhesion stress of surfaces ( $\sigma_0^* < 0.3\sigma_b$ ).

The results obtained demonstrate the key role of the dissipation channel associated with plastic deformation of the material in the realization of the regime of intense adhesive wear. This is confirmed by the results of parametric study of the influence of the yield strength of the material (for the same value of the strain hardening coefficient) on the wear regime. It was established that the change of the yield strength in wide limits practically does not influence on the *critical* value of the adhesion stress at which the transition is observed from the *low* to *high* wear regime given that the elastic energy dissipation power (the  $K_e$  value) remains unchanged. Thus, the wear regime is determined by the energy dissipation power by the mechanisms of plastic deformation rather than by the total work of inelastic deformation of the material with other conditions remaining the same.



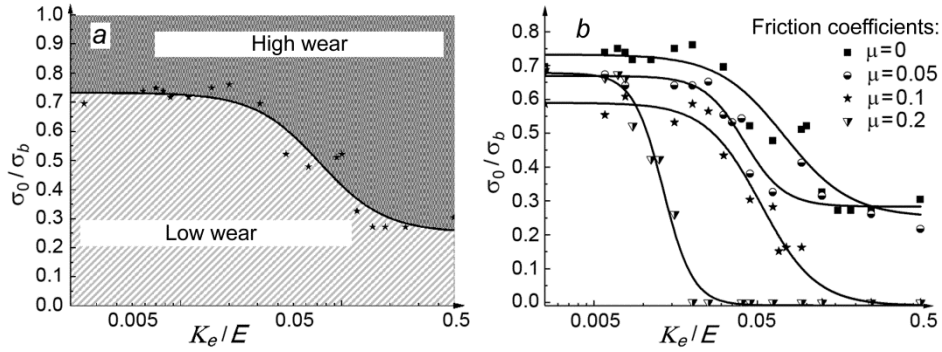


Fig. 5. Typical dependence of the location of the boundary between the areas of low and high wear of microasperities on the value of the strain hardening coefficient  $K_e$  for the dry friction coefficient  $\mu = 0$  (a) and profiles of the boundary for the indicated  $\mu$  values (b). Here symbols show the location of the boundary from the results of computer simulation and the solid curves show the approximating sigmoid.

It is well known that the special features of the contact interaction of microasperity surfaces are determined by processes on different scale levels. The effective account for the influence of underlying scales is traditionally carried out by means of introduction of the dry friction coefficient as the parameter characterizing the elastic energy dissipation intensity on the scales that are by several orders of magnitude less than the characteristic scale of the examined contact area in the mathematical contact model. This allows qualitative consideration of the contacting surfaces of microasperities as multilevel systems to be carried out.

The parametric study of the influence of the dry friction coefficient  $\mu$  on the wear regime of microasperities demonstrated that the increase of  $\mu$  leads to the decrease of the *threshold* adhesion stress  $\sigma_0^*$  (Fig. 5b) given that other mechanical characteristics remained unchanged. In this case, the sigmoid character of the dependence  $\sigma_0^*(K_e)$  remained unchanged. The above-indicated character of the influence of the friction coefficient is explained as follows. The increase of the dry friction on the contact spots of microasperities leads to an increase in the relative shear resistance force of the contacting surfaces and hence, to an increase in the shear stress. This promotes the beginning of plastic deformation of the material at smaller values of the relative displacement on the contact spot, increase of the elastic energy dissipation due to the plastic deformation of the material, and fast exhaustion of the dissipation ability of the channel. As a result, the wear regime changes from the low to high wear at smaller values of the strain hardening coefficient, and the boundary between the regimes is displaced to the left along the abscissa (Fig. 5b).

### 3. DISCUSSION OF RESULTS

As demonstrated above, the threshold value of the adhesion stress of surfaces  $\sigma_0^*$  (and the adhesion work force  $w_{adh}^* = \sigma_0^* \delta$ ), subdividing the regimes of low intensive and high wear of microasperities in tangential contact is a sigmoid function of the strain hardening coefficient of the material. The logistic form of the dependence between the parameters is characteristic for systems whose behavior is determined by a competition between the two factors. In this case, the location of the transition boundary between the wear regimes is determined by the competition between the processes of elastic energy dissipation during plastic deformation of the material and the dissipation at the expense of the adhesion work force.

For materials characterized by the physicomaterial response close to that of the brittle ones and hence, by relatively large values of the strain hardening coefficient, the high wear regime starts already at sufficiently low values of the adhesion force/work. This is due to the fact that at low elastic energy dissipation intensity during plastic

deformation, the critical elastic energy of the material  $w_{\text{elast}}^{\text{crit}}$  and the channel involving dissipation associated with formation of discontinuities are fast reached. This makes the separation of fragments of the material possible already at low (in comparison with the strength) adhesion stress. With increasing dry friction coefficient that is a factor provoking an increase in the shear stress on contact spots, the high wear regime may be observed even in the limiting case of zero adhesion stress (see curves for  $\mu = 0.1$  and  $0.2$  in Fig. 5b).

For the plastic materials characterized by low strain hardening coefficients, the interaction of microasperities is accompanied by the intensive plastic deformation in the contact area and hence dissipation of a larger portion of the mechanical energy arriving to the contact area under loading. Under such conditions, of crucial importance for transition to the high wear regime becomes the attraction of the additional factor providing the increase of the mechanical energy stored in the microasperities. This factor is the adhesive interaction of the surfaces. For  $K_d/E \ll 1$ , the influence of the given factor becomes significant when the adhesion stress is comparable with the strength. Note that the influence of the friction coefficient on the wear regime turns out to be the weaker the closer the material response to that of the ideally plastic material. This is due to the fact that the plastic deformation of the surface layer leads to smoothing of the surface and thereby to a decrease in the absolute value of the friction force (in other words, to the decrease of the contribution of dry friction to the behavior of the surface layer).

## CONCLUSIONS

The results obtained in this work have confirmed the competitive character of two factors that determine the wear regime, namely, the adhesion force and the strain hardening coefficient (which in a broader sense can be treated as the plastic deformability of the material). In this case, the friction coefficient whose value is determined by the processes of elastic energy dissipation at lower lying scale levels of the contacting surfaces is the factor promoting the increase of the wear rate, given that other factors remain the same. This fact is associated with the increase of the tangential force of response on the contact spot and hence with the increase of the stress intensity.

One of the important factors that influence the location of the boundary between the wear regimes (the  $\sigma_0^*$  value) is the shape of the microasperity surface. This is due to the influence of the shape on the stress concentration at the bases of the microasperities and in the contact area that has manifested, in particular, in the occurrence of the form factor in the relationship between the critical value of the work of adhesion forces and the critical value of the elastic energy [3, 12]. A detailed study of the problem about the influence of the geometry of microasperities and a detailed elaboration of its representation in numerical calculations [33] remain beyond the framework of the present work and require additional study.

Thus, our investigations have shown that the value of the adhesion stress of surfaces in tangential contact is the criterion that determines the wear regime. The threshold character of transition from the low to high wear regime, investigated previously only for nano-size microasperities [3, 11, 12, 14], takes place for microasperities of different scales up to the macroscopic ones. In a wide range of scales, up to submicron ones, the statement about the independence of the threshold adhesion stress on the microasperity size remains valid.

This work was supported in part by the Program of Fundamental Scientific Research of the State Academies of Sciences for 2013–2020 (direction III.23).

## REFERENCES

1. A. I. Vakis, V. A. Yastrebov, J. Scheibert, *et al.*, *Tribol. Int.*, **125**, 169–199 (2018).
2. Q. Li and V. L. Popov, *Phys. Mesomech.*, **21**, 94–98 (2018).
3. R. Aghababaei, D. H. Warner, and J.-F. Molinari, *Proc. Natl. Acad. Sci. U.S.A.*, **114**, 7935–7940 (2017).
4. A. Schirmeisen, *Nat. Nanotechnol.*, **8**, 81–82 (2013).
5. M. Ciavarella and A. Papangelo, *Phys. Mesomech.*, **21**, 59–66 (2018).
6. D. Maugis, *J. Adhes. Sci. Technol.*, **10**, 161–175 (1996).

7. Y. I. Rabinovich., J. J. Adler, A. Ata, *et al.*, *J. Colloid Interface Sci.*, **232**, 10–16 (2000).
8. J. T. Burwell and C. D. Strand, *J. Appl. Phys.*, **23**, 18–28 (1952).
9. J. F. Archard, *J. Appl. Phys.*, **24**, 981–988 (1953).
10. E. Rabinowicz, *Friction and Wear of Materials*, John Wiley & Sons, New York (2013). – P. 125–166.
11. J. Von Lutz, L. Pastewka, P. Gumbsch, and M. Moseler, *Tribol. Lett.*, **63**, Art. 26 (2016).
12. T. Brink and J.-F. Molinari, *Phys. Rev. Mat.*, **3**, Art. 053064 (2019).
13. E. Rabinowicz, *Wear*, **2**, 4–8 (1958).
14. R. Aghababaei, D. H. Warner, and J.-H. Molinari, *Nat. Commun.*, **7**, Art. 11816 (2016).
15. J. Zhong, R. Shakiba, and J. B. Adams, *J. Phys. D*, **46**, Art. 055307 (2013).
16. K. P. Zolnikov, D. S. Kryzhevich, and A. V. Korchuganov, *Lett. Mater.*, **9**, 197–201 (2019).
17. S. G. Psakhie, K. P. Zolnikov, D. S. Kryzhevich, and A. V. Korchuganov, *Sci. Rep.*, **9**, Art. 3867 (2019).
18. L. Jing and O. Stephansson, *Fundamentals of Discrete Element Method for Rock Engineering: Theory and Applications*, Elsevier, Amsterdam (2007).
19. D. O. Potyondy and P. A. Cundall, *Int. J. Rock. Mech. Min. Sci.*, **41**, 1329–1364 (2004).
20. N. L. Savchenko, A. V. Filippov, S. Yu. Tarasov, *et al.*, *Friction*, **6**, 323–340 (2018).
21. S. Psakhie, E. Shilko, A. Smolin, *et al.*, *Frattura Integr. Strutt.*, **24**, 59–91 (2013).
22. E. V. Shilko, S. G. Psakhie, S. Schmauder, *et al.*, *Comp. Mater. Sci.*, **102**, 267–285 (2015).
23. S. G. Psakhie, A. V. Dimaki, E. V. Shilko, and S. V. Astafurov, *Int. J. Num. Meth. Eng.*, **106**, 623–643 (2016).
24. S. Wu and X. Xu, *Rock Mech. Rock Eng.*, **29**, 1813–1830 (2016).
25. N. Bicanic, in: *Encyclopaedia of Computational Mechanics*, E. Stein, R. de Borst, and T. R. J. Hughes, eds., John Wiley & Sons, Glasgow (2017), pp. 1–38.
26. M. L. Wilkins, *Computer Simulation of Dynamic Phenomena*, Springer Verlag, Berlin (1999).
27. F. M. Borodich, *Adv. Appl. Mech.*, **47**, 225–366 (2014).
28. M. Inoue, in: *Advanced Adhesives in Electornics. Materials, Properties and Applications*, M. O. Alam and C. Bailey, eds., Woodhead Publishing, Cambridge (2011), pp. 157–198.
29. D. S. Dugdale, *J. Mech. Phys. Solids*, **8**, 100–104 (1960).
30. D. J. Maugis, *J. Colloid Interface Sci.*, **150**, 243–269 (1992).
31. I. V. Dudkin, E. V. Shilko, and A. V. Dimaki, *AIP Conf. Proc.*, **2051**, Art. 020069 (2018).
32. A. M. Glezer, *Bull. RAS. Physics*, **71**, No. 12, 1722 (2007).
33. A. Dimaki, E. Shilko, S. Psakhie, and V. Popov, *Facta Univ. Mech. Eng.*, **16**, 41–50 (2018).